Journal of Photochemistry and Photobiology A: Chemistry 218 (2011) 219–225

Contents lists available at ScienceDirect

Journal of Photochemistry and Photobiology A: Chemistry

journal homepage: www.elsevier.com/locate/jphotochem

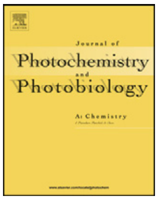

Synthesis, characterization and application of *trans*-D–B–A-porphyrin based dyes in dye-sensitized solar cells

Kalyan Kumar Pasunooti[a,1], Jun-Ling Song[a,1], Hua Chai[a], Pitchamuthu Amaladass[a], Wei-Qiao Deng[b,*], Xue-Wei Liu[a,**]

[a] *Division of Chemistry and Biological Chemistry, School of Physical & Mathematical Sciences, Nanyang Technological University, Singapore 637371, Singapore*
[b] *Dalian Institute of Chemical Physics, Chinese Academy of Sciences, Dalian 116023, PR China*

ARTICLE INFO

Article history:
Received 15 October 2010
Received in revised form
26 December 2010
Accepted 6 January 2011
Available online 13 January 2011

Keywords:
Dye-sensitized solar cells
Porphyrin
Push–pull
Charge-separation
Aggregation

ABSTRACT

A series of metal-free *trans*-D–B–A porphyrin dyes have been synthesized and characterized as photosensitizers for dye-sensitized solar cells (DSSCs). These dye molecules contain a porphyrin unit as a π-bridge, a substituted phenyl group as an electron donor and cyanoacrylic acid or carboxylic acid group as an electron acceptor (anchoring groups). This phenomenon is more pronounced for porphyrins (Dye **4** and Dye **5**) that have conjugated diphenyl aniline at the opposite side of the anchoring group. A solar conversion efficiency of 2.38% has been achieved with a short circuit current (J_{sc}) of 7.63 mA/cm^2, an open circuit voltage (V_{oc}) of 0.613 V and a fill factor (*ff*) of 51.0% for Dye **5** under standard global AM 1.5 solar irradiation. Results of time-dependent density functional theory (TD-DFT) calculations on these five organic dyes support the electrochemical data.

1. Introduction

Since past few years there has been considerable attention in photo-active molecules to convert solar energy into electrical power. Dye-sensitized solar cells (DSSCs) have been paid much attention due to the relatively high solar energy conversion and potentially low cost [1–3]. Organic or inorganic dye sensitizers have been found as one of the most important tool for DSSCs to get high conversion efficiency. In this connection, several research groups have been devoted to explore the efficient dyes to improve the cell performance. Commonly, transition polypyridine ruthenium complexes such as **N3** [1,4], **N719** [1,4,5], and **Z907** [6,7] shows the overall conversion efficiency reaching up to 11% under 100 mW/cm^2 illumination of simulated solar light. In recent years, the interests in organic dyes as substitutes of noble metal complexes are increasing due to many advantages, such as diversity of molecular structures, high molar extinction co-efficient, simple synthesis as well as low cost and environmental issues. Metal-free organic dyes have been developed and showed good performance in solar cells [8–17]. More recently, we have reported the design and synthesis of novel donor–acceptor aryl/hetero-arylethyne bridged dyes for photovoltaic performances of DSSCs [18].

Among all organic dyes, porphyrins and their derivatives have been considered as potential photosensitizers in DSSCs because they possess an intense Soret band at 400–450 nm and moderate Q bands at 500–650 nm [19–25]. However, porphyrin dyes showed low efficiency compared to Ru dyes for DSSCs due to their insufficient light-harvesting properties in the visible region. To improve the performance of porphyrin dyes, porphyrins with extended π-conjugation and efficient anchoring groups have been designed and this led to better photo-voltaic performance. Porphyrin based push–pull chromophores shows large conjugation and strong electronic interaction between chromophores as previously reported [26–28], and this type of sensitizers can facilitate the direction of electron injection, reduce the aggregation on a TiO_2 surface, tune the level of the excited state and increase the electron coupling between the sensitizers and the semiconductor [11]. Based on this hypothesis, we investigate a series of unsymmetrical *trans*-D–B–A-porphyrin based dye molecules (D = donor, B = bridge, A = acceptor) with different donating group substituent on the opposite side of the acceptor to be used for dye sensitized solar cells (DSSCs). Here, we report the synthesis, electrochemical and photovoltaic properties of a series of metal-free porphyrin sensitizers based on the donor–acceptor porphyrin chromophores and their molecular structures were shown in Fig. 1.

---

[*] Corresponding author.
[**] Corresponding author. Tel.: +65 6316 8901.
E-mail addresses: dengwq@dicp.ac.cn (W.-Q. Deng), xuewei@ntu.edu.sg (X.-W. Liu).
[1] These authors contributed equally to this work.

1010-6030/$ – see front matter © 2011 Elsevier B.V. All rights reserved.
doi:10.1016/j.jphotochem.2011.01.003

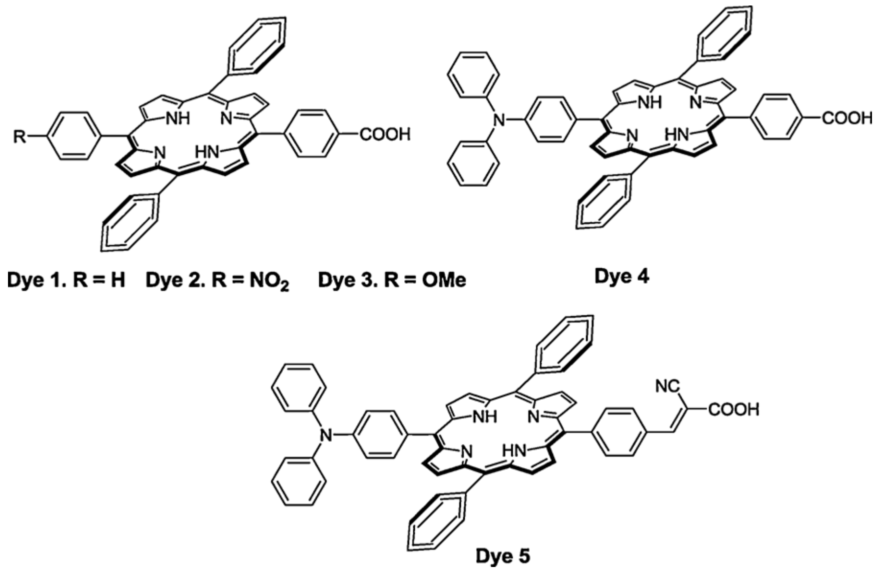

Fig. 1. Structures of the porphyrin dyes (Dyes **1**–**5**).

2. Experimental

2.1. Material and instrumentation

All chemicals were obtained from commercial sources and used without further purification. Unless otherwise noted, all reactions were carried out in oven-dried glassware under an atmosphere of nitrogen. Solvents and reagents were purified according to the standard procedure prior to use. Product purification by flash column chromatography was accomplished using silica gel 60 mesh. Technical grade solvents were used for chromatography and distilled prior to use. NMR spectra were recorded at room temperature on a 300 MHz Bruker ACF 300, 400 MHz Bruker DPX 400 and 500 MHz Bruker AMX 500 NMR spectrometers, respectively. The residual solvent signals were taken as the reference (7.26 ppm for ^{1}H NMR spectroscopy). Infrared spectra were recorded on a Bio-RAD FTS 165 FT-IR Spectrometer and reported in cm^{-1}. Samples were prepared in thin film technique. HRMS (ESI) spectra were recorded on a Finnigan/MAT LCQ quadrupole ion trap mass spectrometer, coupled with the TSP4000 HPLC system and the Crystal 310 CE system. Absorption spectrums were measured on JASCO V-670 UV–Vis-Near IR spectrophotometer and photoluminescence analyses were performed on a Cary Eclipses fluorescence spectrometer.

2.2. Synthesis

2.2.1. 2,2′-(Phenylmethylene)bis(1H-pyrrole) (*1*) [29]

Distilled pyrrole (60.0 mL, 866.0 mmol) and benzaldehyde (3.50 mL, 34.6 mmol) were added to a dry round-bottomed flask and degassed with a stream of nitrogen for 5 min. TFA (0.26 mL, 3.46 mmol) was add to the reaction mixture, which stirred under nitrogen atmosphere at room temperature for 5 min and then quenched with 0.1 M NaOH. The reaction mixture was extracted with ethyl acetate. The combined organic phase was washed with brine, dried over anhydrous $NaSO_4$ and concentrated under reduced pressure to provide a residue. It was purified by flash column chromatography to give intermediate **1** as a pale yellow solid.

2.3. General experimental procedure for porphyrins *6*, *7*, *8* and *9*

Aldehyde (1.17 mmol) and methyl 4-formylbenzoate (1.17 equiv) were added to a dry round-bottomed flask and placed under high vacuum. Propionic acid (0.05 M) was added to the reaction mixture under nitrogen atmosphere at room temperature. This reaction mixture was heated to reflux and 5-phenyldipyrromethane **1** (2.25 mmol) in propionic acid (0.25 M) was added slowly over 20 min. The mixture was refluxed for 2 h and then the crude product was evaporated to dryness under vacuum. The black solid was purified by column chromatography on silica gel to give the desired porphyrin product.

2.3.1. 5,15-Bisphenyl-10-(4-nitro)phenyl-20-(4-methoxycarbonyl phenyl)-porphyrin (*6*)

Purification of the crude product by flash column chromatography on silica gel gave purple color solid compound **6** (240 mg, 15%): ^{1}H NMR (500 MHz, $CDCl_3$): δ in ppm = 8.88–8.85 (m, 6H), 8.79 (d, J = 4.6 Hz, 2H), 8.44 (dd, J = 6.5 and 1.7 Hz, 2H), 8.30 (d, J = 1.3 Hz, 2H), 8.22 (dd, J = 7.6 and 1.4 Hz, 6H), 7.81–7.73 (m, 8H), 4.11 (s, 3H), −2.77 (s, 2H). ^{13}C NMR (100 MHz, $CDCl_3$): δ in ppm = 167.3, 146.9, 141.9, 134.5, 134.5, 129.6, 127.9, 127.8, 126.7, 120.6, 118.9, 52.4. IR ($CHCl_3$): ν_{max} = 3030, 1660, 1210, 758 cm^{-1}. LC–MS (ESI): (M+1): 718.

2.3.2. 5,10,15-Trisphenyl-20-(4-methoxycarbonylphenyl) porphyrin (*7*)

Purification of the crude product by flash column chromatography on silica gel gave purple color solid compound **7** (400 mg, 14%): ^{1}H NMR (500 MHz, $CDCl_3$): δ in ppm = 8.87–8.85 (m, 6H), 8.80 (d, J = 4.6 Hz, 2H), 8.44 (d, J = 8.1 Hz, 2H), 8.31 (d, J = 8.1 Hz, 2H), 8.22 (dd, J = 7.6 and 1.4 Hz, 6H), 7.79–7.73 (m, 9H), 4.11 (s, 3H), −2.76 (s, 2H). IR ($CHCl_3$): ν_{max} = 3025, 2200, 1653, 760 cm^{-1}. HRMS (ESI): m/z: calcd for $C_{46}H_{33}N_4O_2$: 673.2604 $[M]^+$; found: 673.2608.

2.3.3. 5,15-Bisphenyl-10-(4-methoxy)phenyl-20-(4-methoxy carbonylphenyl)-porphyrin (*8*)

Purification of the crude product by flash column chromatography on silica gel gave purple color solid compound **8** (240 mg, 15%): ^{1}H NMR (500 MHz, $CDCl_3$): δ in ppm = 8.91–8.80 (m, 6H), 8.81 (d, J = 4.3 Hz, 2H), 8.45 (d, J = 7.8 Hz, 2H), 8.32 (d, J = 7.8 Hz, 2H), 8.23 (d, J = 6.7 Hz, 4H), 8.14 (d, J = 8.1 Hz, 2H), 7.79–7.74 (m, 6H), 7.29 (d, J = 8.2 Hz, 2H), 4.12 (s, 3H), 4.09 (s, 3H), −2.73 (s, 2H). ^{13}C NMR (100 MHz, $CDCl_3$): δ in ppm = 167.3, 159.4, 147.1, 142.1, 135.6, 134.6, 134.5, 134.4, 129.5, 127.9, 127.7, 126.7, 120.5, 120.3, 118.3, 112.2, 55.5, 52.4. IR ($CHCl_3$): ν_{max} = 3030, 2350, 1650, 758 cm^{-1}.

HRMS (ESI): *m*/*z*: calcd for $C_{47}H_{35}N_4O_3$: 703.2709 $[M]^+$; found: 703.2708.

*2.3.4. 5,15-Bisphenyl-10-(4-diphenylamino)phenyl-20-(4-methoxy carbonylphenyl)-porphyrin (**9**)*

Purification of the crude product by flash column chromatography on silica gel gave purple color solid compound **9** (500 mg, 13%): ^{1}H NMR (500 MHz, $CDCl_3$): δ in ppm = 9.03 (d, J = 4.6 Hz, 1H), 8.94–8.84 (m, 4H), 8.82–8.76 (m, 2H), 8.46 (d, J = 6.4 Hz, 2H), 8.33 (d, J = 8.1 Hz, 2H), 8.25–8.24 (m, 4H), 8.10 (d, J = 6.6 Hz, 1H), 7.83–7.75 (m, 6H), 7.70 (d, J = 7.0 Hz, 1H), 7.48 (d, J = 6.6 Hz, 1H), 7.44 (d, J = 3.4 Hz, 5H), 7.37 (t, J = 6.3 Hz, 2H), 7.21–7.15 (m, 4H), 7.04 (d, J = 8.6 Hz, 1H), 4.12 (s, 3H), −2.71 (s, 2H). ^{13}C NMR (100 MHz, $CDCl_3$): δ in ppm = 167.4, 147.8, 147.1, 142.1, 135.6, 134.6, 129.5, 127.9, 127.8, 126.7, 124.9, 123.3, 121.2, 120.3, 118.3, 52.4. IR ($CHCl_3$): ν_{max} = 3020, 2405, 1550, 1215, 755 cm^{-1}. HRMS (ESI): *m*/*z*: calcd for $C_{58}H_{42}N_5O_2$: 840.3339 $[M]^+$; found: 840.3336.

*2.4. General experimental procedure for porphyrin Dyes **1**–**4***

The desired porphyrin methyl ester (0.29 mmol) was dissolved in 50 mL of isopropanol. KOH (2.9 mmol) dissolved in water (0.02 M) was added to this solution and the reaction mixture was refluxed for 6 h. After cooling to room temperature, the mixture was neutralized with 1 M HCl solution and the resulting suspension was extracted with chloroform. The organic layer was washed with water, dried and evaporated to dryness. The crude product was purified by column chromatography on silica gel to give the desired porphyrin product.

*2.4.1. 5,10-Bisphenyl-10-(4-nitro)phenyl-20-(4-carboxymethyl phenyl)-porphyrin (Dye **1**)*

Purification of the crude product by flash column chromatography on silica gel gave compound Dye **1** (185 mg, 94%): ^{1}H NMR (500 MHz, $CDCl_3$): δ in ppm = 8.88–8.85 (m, 6H), 8.79 (d, J = 4.6 Hz, 2H), 8.44 (dd, J = 6.5 and 1.7 Hz, 2H), 8.30 (d, J = 1.3 Hz, 2H), 8.22 (dd, J = 7.6 and 1.4 Hz, 6H), 7.81–7.73 (m, 8H), −2.77 (s, 2H). IR ($CHCl_3$): ν_{max} = 3018, 2399, 1670, 1521, 1261, 1215, 756 cm^{-1}. HRMS (ESI): *m*/*z*: calcd for $C_{45}H_{30}N_5O_4$: 704.7447 $[M]^+$; found: 704.7441.

*2.4.2. 5,10,15-Trisphenyl-20-(4-carboxymethylphenyl)-porphyrin (Dye **2**)*

Purification of the crude product by flash column chromatography on silica gel gave porphyrin Dye **2** (180 mg, 92%): ^{1}H NMR (500 MHz, $CDCl_3$): δ in ppm = 8.87–8.81 (m, 8H), 8.51 (d, J = 7.6 Hz, 2H), 8.35 (d, J = 7.7 Hz, 2H), 8.22 (d, J = 6.2 Hz, 2H), 8.22 (d, J = 6.2 Hz, 6H), 7.77–7.76 (m, 9H), −2.77 (s, 2H). IR ($CHCl_3$): ν_{max} = 3010, 1670, 1530, 1260, 1210 cm^{-1}. HRMS (ESI): *m*/*z*: calcd for $C_{45}H_{31}N_4O_2$: 659.2447 $[M]^+$; found: 659.2435.

*2.4.3. 5,10-Bisphenyl-10-(4-methoxy)phenyl-20-(4-carboxymethyl phenyl)-porphyrin (Dye **3**)*

Purification of the crude product by flash column chromatography on silica gel gave porphyrin Dye **3** (190 mg, 97%): ^{1}H NMR (500 MHz, $CDCl_3$): δ in ppm = 8.91–8.80 (m, 6H), 8.81 (d, J = 4.3 Hz, 2H), 8.45 (d, J = 7.8 Hz, 2H), 8.32 (d, J = 7.8 Hz, 2H), 8.23 (d, J = 6.7 Hz, 4H), 8.14 (d, J = 8.1 Hz, 2H), 7.79–7.74 (m, 6H), 7.29 (d, J = 8.2 Hz, 2H), 4.09 (s, 3H), −2.73 (s, 2H). IR ($CHCl_3$): ν_{max} = 3018, 2399, 1653, 1215, 758 cm^{-1}. HRMS (ESI): *m*/*z*: calcd for $C_{46}H_{33}N_4O_3$: 689.2553 $[M]^+$; found: 689.2551.

*2.4.4. 5,15-Bisphenyl-10-(4-diphenylamino)phenyl-20-(4-carboxy methylphenyl)-porphyrin (Dye **4**)*

Purification of the crude product by flash column chromatography on silica gel gave porphyrin Dye **4** (194 mg, 98%): ^{1}H NMR (500 MHz, $CDCl_3$): δ in ppm = 9.04–9.03 (m, 1H), 8.92–8.86 (m, 4H), 8.84 (d, J = 4.6 Hz, 2H), 8.58 (d, J = 7.9 Hz, 2H), 8.40 (d, J = 6.1 Hz, 2H), 8.27–8.25 (m, 5H), 8.11 (d, J = 5.1 Hz, 1H), 7.83–7.79 (m, 7H), 7.49 (d, J = 8.2 Hz, 1H), 7.45 (d, J = 4.2 Hz, 5H), 7.28 (d, J = 7.5 Hz, 4H), 7.27–7.16 (m, 2H), −2.72 (s, 2H). IR ($CHCl_3$): ν_{max} = 3015, 2400, 1670, 1560, 1220 cm^{-1}. HRMS (ESI): *m*/*z*: calcd for $C_{57}H_{40}N_5O_2$: 826.3182 $[M]^+$; found: 826.3180.

*2.4.5. 5,15-Bisphenyl-10-(4-diphenylamino)phenyl-20-(4-hydroxy methylphenyl)-porphyrin (**10**)*

Porphyrin **9** (50 mg, 0.06 mmol) was dissolved in 2 mL of THF at 0 °C. After addition of $LiAlH_4$ (6.8 mg, 0.18 mmol), the mixture was allowed to reach room temperature and stirred for 3 h. After being quenched by water, the mixture was stirred for further 10 min. The solvent was removed by using a rotary evaporator, and the residue was dissolved in dichloromethane and passed through the filter paper. The filtrate was washed with water and dried over Na_2SO_4. Evaporation of the solvent afforded purple solid, which was purified by silica gel column chromatography to give desired alcohol **10** (46 mg, 95%) as a purple solid. ^{1}H NMR (500 MHz, $CDCl_3$): δ in ppm = 9.02 (d, J = 4.4 Hz, 2H), 8.89–8.85 (m, 6H), 8.22 (dd, J = 12.0 and 7.4 Hz, 6H) 8.09 (d, J = 8.2 Hz, 2H), 7.79–7.73 (m, 8H), 7.47 (d, J = 8.3 Hz, 2H), 7.42–7.40 (m, 8H), 7.16–7.13 (m, 2H), 5.04 (d, J = 8.1 Hz, 2H), 1.97 (t, J = 5.6 Hz, 1H) −2.71 (s, 2H). ^{13}C NMR (125 MHz, $CDCl_3$): δ in ppm = 147.8, 147.5, 142.2, 135.8, 135.6, 134.7, 130.9, 129.5, 127.7, 126.7, 125.3, 124.9, 123.3, 121.2, 120.3, 120.1, 65.4. IR ($CHCl_3$): ν_{max} = 3020, 2390, 1558, 1530, 756 cm^{-1}. IR ($CHCl_3$): ν_{max} = 3018, 2399, 1558, 1506, 1215, 756 cm^{-1}. HRMS (ESI): *m*/*z*: calcd for $C_{57}H_{42}N_5O$: 812.3389 $[M]^+$; found: 812.3387.

*2.4.6. 5,15-Bisphenyl-10-(4-diphenylamino)phenyl-20-(4-formyl phenyl)-porphyrin (**11**)*

Porphyrin **10** (30 mg, 0.04 mmol) was dissolved in 2 mL of dichloromethane and cooled to 0 °C. After addition of MnO_2 (6.3 mg, 0.07 mmol), the mixture was allowed to reach room temperature and stirred for 6 h. The reaction mixture was then dissolved in excess dichloromethane and passed through the celite. The filtrate was washed with water and dried over Na_2SO_4. Evaporation of the solvent afforded purple solid, which was purified by silica gel column chromatography to give desired aldehyde **11** (27 mg, 91%) as a purple solid. ^{1}H NMR (400 MHz, $CDCl_3$): δ in ppm = 10.36 (s, 1H), 9.05 (d, J = 4.7 Hz, 2H), 8.91 (d, J = 4.7 Hz, 4H), 8.80 (d, J = 4.8 Hz, 2H), 8.42 (d, J = 5.2 Hz, 2H), 8.39–8.24 (m, 6H), 8.10 (d, J = 8.3 Hz, 2H), 7.83–7.75 (m, 6H), 7.49–7.47 (m, 10H), 7.19–7.14 (m, 2H), −2.68 (s, 2H). ^{13}C NMR (100 MHz, $CDCl_3$): δ in ppm = 192.4, 148.7, 147.8, 147.6, 142.0, 135.6, 135.2, 134.6, 129.5, 128.0, 127.8, 126.7, 125.0, 123.4, 121.1, 120.9, 120.5, 117.8. IR ($CHCl_3$): ν_{max} = 3020, 2390, 1550, 1516, 1215, 756 cm^{-1}. HRMS (ESI): *m*/*z*: calcd for $C_{57}H_{40}N_5O$: 810.3233 $[M]^+$; found: 810.3234.

*2.4.7. 5,15-Bisphenyl-10-(4-diphenylamino)phenyl-20-[4-(2-carboxy-2-cynovinyl)phenyl]-porphyrin (Dye **5**)*

2-Cynoacetic acid (25 mg, 0.3 mmol) and piperidine (60 μL, 0.6 mmol) were dissolved in acetonitrile (2 mL) and placed under nitrogen atmosphere at room temperature. Porphyrin **11** in acetonitrile (1 mL) was then added to the reaction mixture and heated to reflux for 4 h. After cooling to room temperature, the mixture was washed with 2 M aqueous HCl and extracted with chloroform. The organic phase was collected and dried over Na_2SO_4. After removal of solvent, the crude product was purified on the silica gel column to afford the porphyrin Dye **5** as a purple solid (45 mg, 85%). ^{1}H NMR (400 MHz, $CDCl_3$): δ in ppm = 10.74 (bs, 1H), 8.88 (s, 2H), 8.74–8.71 (m, 6H), 8.40–8.38 (m, 2H), 8.30–8.28 (m, 2H), 8.15–8.10 (m, 4H), 7.97 (d, J = 8.0 Hz, 2H), 7.71–7.67 (m, 6H), 7.34 (d, J = 8.3 Hz, 2H), 7.71–7.67 (m, 8H), 7.03–6.99 (m, 2H), −2.75 (s, 2H). IR ($CHCl_3$): ν_{max} = 3010, 2350, 1520, 756 cm^{-1}. HRMS (ESI): *m*/*z*: calcd for $C_{60}H_{41}N_6O_2$: 877.3291 $[M]^+$; found: 877.3289.

2.5. Calculation method

All calculations were performed with the Gaussian 03 program package [30]. The geometries of molecules *in vacuo* were optimized using density functional theory (DFT) with the B3LYP density functional and the 6-31G* basis set. The time-dependent DFT (TD-DFT) at the level of B3LYP/6-31G* was carried out to study the excited state of selected molecules [31]. The 20 lowest spin-allowed singlet transitions were involved to simulate the absorption spectra. TD-DFT calculations were performed in tetrahydrofuran (THF) solution (C-PCM model) with geometries obtained *in vacuo*. The contribution of singlet excited state configurations to each electronic transition and the simulated absorption spectra of the porphyrin analogues and graphical molecular orbital were generated with the Gauss View software program (version 3.09) [30].

2.6. Electrochemistry

Electrochemistry was characterized with Eco Chemie Autolab PGSTAT 100 with an ADC fast scan generator. Planar Pt disks (1 mm diameter) were used as working electrodes in conjunction with a Pt auxiliary electrode. An Ag/Ag^+ reference electrode was connected to the test solution *via* a salt bridge containing 0.2 M Bu_4NPF_6 in THF. Accurate potentials were obtained using ferrocene as an internal standard. All potentials reported herein are *vs*. $FeCp_2/FeCp_2^+$ = 0.41 V.

2.7. Preparation of porphyrin sensitized TiO_2 electrode

Conducting glasses (SnO_2:F, FTO, 15 Ω/sq, Solaronix) were washed with 0.1 M HCl and isopropyl alcohol and then the glass was treated with 40 mM $TiCl_4$ aqueous solution at 70 °C for 40 min following a literature procedure. The 10.0 μm thick films of nanocrystalline TiO_2 (Ti-Nanoxide T/SP, Solaronix) were deposited onto the side of conducting layer of FTO by doctor blading. TiO_2 substrates were sintered at 500 °C for 30 min in air and then in immersed 40 mM $TiCl_4$ aqueous solution at 70 °C for 40 min. Then the TiO_2 plates were dipped into 0.5 mM dye solution in THF and left for 2 h at 50 °C, and taken out and rinsed with methanol. A 400 Å Pt fabricated by e-beam evaporation on a commercial indium tin oxide glass as the counter electrode was then clipped onto the top of the TiO_2 working electrode to form the test cell. The two electrodes separated by 50 μm thermal-plastic Suryln spacers were bonding together, and the electrolyte (EL-HPE from dyesol) was introduced between the electrodes by capillary action.

2.8. Photovoltaic characterization

A Sun 2000 solar simulator light source (Abet-technologies, U.S.A.) was used to give an irradiance of 100 mW cm^{-2} (the equivalent of one sun at air mass (AM) 1.5) at the surface of solar cells. The current–voltage characteristics of the cell under these conditions were obtained by applying external potential bias to the cell and measuring the generated photocurrent with a Keithley model 2440 digital source meter (Keithley, U.S.A.). This process was fully automated using lab tracer software.

2.9. Electrochemistry

Eco Chemie Autolab PGSTAT 100 with an ADC fast scan generator. Working electrodes were 1 mm diameter planar Pt disks, used in conjunction with a Pt auxiliary electrode and an Ag/Ag^+ reference electrode was connected to the test solution *via* a salt bridge containing 0.2 M Bu_4NPF_6 in THF. Accurate potentials were obtained using ferrocene as an internal standard. All potentials reported herein are *vs*. $FeCp_2/FeCp_2^+$ = 0.41 V.

3. Results and discussion

3.1. Synthesis of porphyrin dyes

The structures of the five porphyrin dye sensitizers were presented in Fig. 1. And the synthetic pathway of porphyrin Dyes **1**–**5** was shown in Scheme 1. The syntheses involve two important steps to get desired porphyrin dyes such as (1) condensation of an appropriate aldehydes with dipyrrophenylmethane unit to afford the porphyrins as precursors, and (2) subsequent hydrolysis of the precursor porphyrins with KOH afforded the corresponding porphyrin Dyes **1**–**4** [29]. Porphyrins (**6**, **7**, **8** and **9**) were synthesized by employing modified Aldler–Longo method [32]. This method involves cross condensation of phenyl dipyrromethane (**1**) with different substituted aldehydes (**2**–**5**) followed by basic hydrolysis afforded the desired products (Dyes **1**–**4**). Synthesis of the acrylic acid derivative Dye-**5** was achieved *via* $LiAlH_4$ reduction of ester **9** to alcohol **10** using standard procedure. MnO_2 oxidation of **10** to alde-

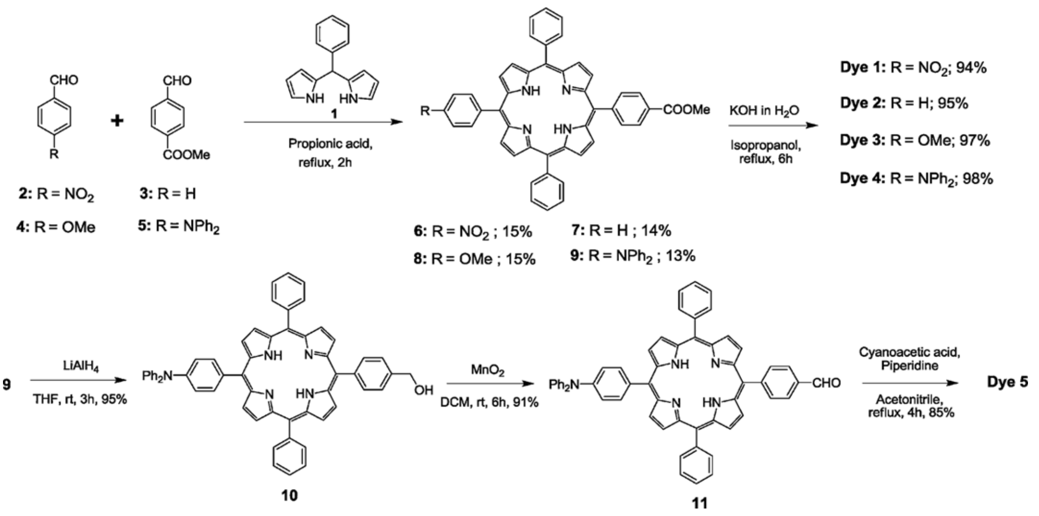

Scheme 1. Synthesis of porphyrin dyes (Dyes **1**–**5**).

hyde **11**, followed by subsequent condensation with cyanoacetic acid to give the desired porphyrin product (Dye-**5**). These porphyrin dyes were fully characterized by spectroscopic analyses including NMR, FT-IR and mass spectra.

3.2. Absorption properties in solution and on TiO_2 film

The UV–vis spectra of the porphyrins (Dyes **1**–**5**) in THF are shown in Fig. 2 and the related absorption maxima and extinction coefficients for the Soret- and Q-bands of the porphyrins are provided in Table S1. The bands between 400 and 650 nm are due to π–π^* absorptions of the conjugation. The dye with a cyanoacrylic acid anchoring group (Dye **5**) shows broader absorption than the carboxylic ones (Dyes **1**–**4**) that are red-shifted with respect to the Soret- and Q-bands of porphyrins. The absorption spectra of films show that there are some dyes aggregated on the surface of TiO_2 nanoparticles in accordance with the reported results [9,11]. The emission spectra of porphyrins Dyes **1**–**5** shown in Fig. 3, in THF. The emission maxima (Table S1) show characteristic vibronic bands for Dyes **1**–**5** at around 630 and 675 nm similar to those reported for other porphyrins [19,26].

3.3. Photophysical properties

In this article, we performed DFT and time-depended density functional theory (TD-DFT) calculations to investigate the intramolecular charge separation of the newly synthesized organic dyes (Dyes **1**–**5**). As shown in Fig. 4, in all dye molecules the major portion of the highest occupied molecular orbital (HOMO) is located on the donor moiety and the lowest unoccupied molecular orbital (LUMO) is located on the acceptor and the bridge moieties. The HOMO position can be adjusted by introducing different donor groups; and LUMO can be tuned by installing an acceptor group on the *trans* position of porphyrin ring. Therefore, the band gap of the dye molecule can be reduced through structural modification. This allows broad absorption bands and easy intramolecular charge separation, which eventually improve the high cell performance of DSSCs. As shown in Fig. 4, the calculated HOMO energy level increase in the order $-NO_2 < -H < -OMe < -NPh_2$, and same as LUMO energy level increase in the order of $-COOH \langle -C{=}C(CN)COOH$. These results imply the formation of a charge-separation between the donor and acceptor during photo-induced electron transfer. In addition, For the five dye sensitizers, the HOMO level higher than the reduction potential of electrolyte (I^-/I_3^-, +0.5 V *vs.* NHE) while LUMO level should be more negative than the conduction band of TiO_2 (−0.5 V *vs.* NHE), which indicate that these molecules are suitable as sensitizers in DSSCs. The TD-DFT calculation results of these Dyes **1**–**5** are shown in Table 2 and Table S2. The excitation energies of them indicated that introduction of donor group such as Ph_2N group, acceptor group such as nitro-group and cyanoacetic acid into the dye molecule can significantly increase the oscillator strength of the Soret band and Q-band. In addition, the donor and acceptor moieties also help to decrease the HOMO–LUMO band-gap, which enhances the solar spectral overlap. The two dominating excitation states, originated from HOMO → LUMO and HOMO → LUMO + 1 (Dyes **2**–**5**) and HOMO → LUMO and HOMO − 1 → LUMO (Dye **1**), and their intensities are primarily coincident with the experimental absorptions of these five compounds as shown in Fig. 2a.

The oxidation potential of the Dyes **1**–**5** was determined with cyclic voltammetry. The measurements were performed in THF solution with 0.2 M tetrabutyl ammonium hexafluorophosphate (Bu_4NPF_6). Ferrocene was used as an internal standard at 0.63 V *vs.* NHE (Figure S1). The oxidation potential of Dyes **1**–**5** is 1.09, 1.17, 1.16, 1.21 and 1.22 V *vs.* NHE respectively, which are more positive than that of I^-/I_3^- couple (0.5 V *vs.* NHE) [28]. These results ensure the regeneration of sensitizer radical cations by the electrolyte redox couple. The excited state oxidation potential of Dyes **1**–**5** is −0.95, −0.87, −0.86, −0.70 and −0.69 V respectively, which are more negative than the conduction band (CB) of TiO_2 (−0.5 V *vs.* NHE). Thereby, this provides enough driving force to inject electrons from the excited porphyrin singlet state to the conduction band (CB) of TiO_2 (Table S3) [13,33].

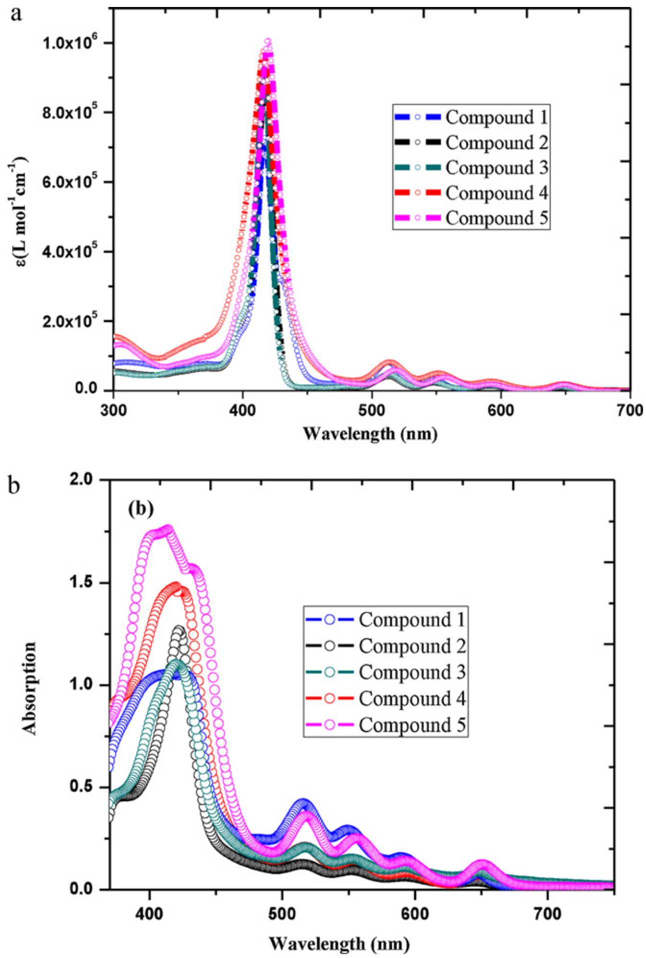

Fig. 2. (a) UV–visible absorption spectra of Dyes **1**–**5** in THF solution. (b) Adsorbed on TiO_2.

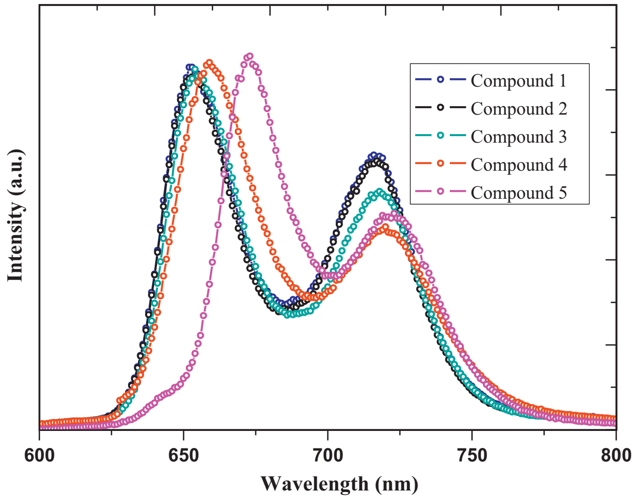

Fig. 3. Emission spectra of Dyes **1**–**5** in THF solution.

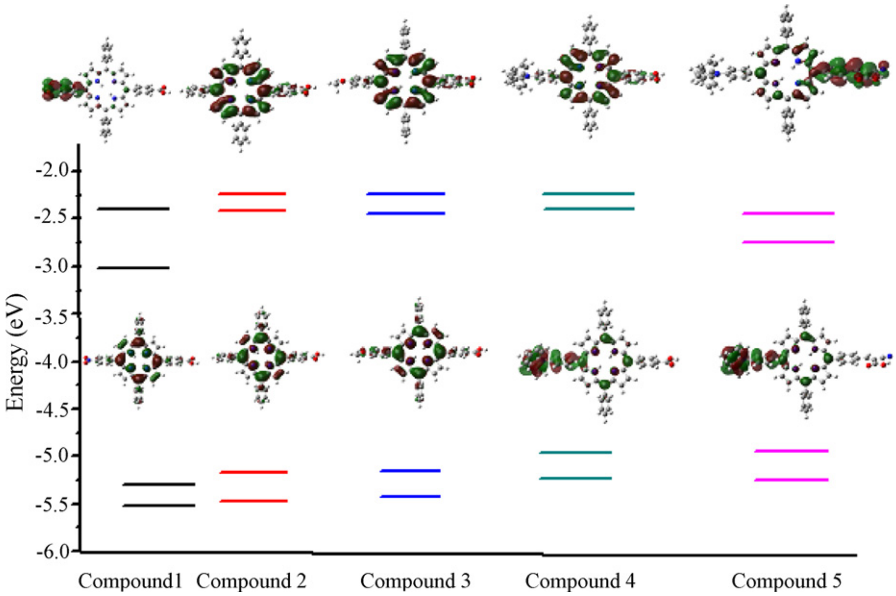

Fig. 4. Molecular orbital diagrams of Dyes **1**–**5**.

Table 1
J–*V* characteristics of the porphyrin sensitizers and **Z907** sensitized solar cell with ionic liquid electrolyte under AM 1.5 irradiation condition.

Electrode	J_{sc} (mA/cm^2)	V_{oc} (V)	*ff* (%)	η (%)
Dye **1**	2.23	0.542	54.9	0.66
Dye **2**	2.90	0.553	55.5	0.89
Dye **3**	4.66	0.563	54.9	1.44
Dye **4**	4.95	0.605	50.8	1.52
Dye **5**	7.63	0.613	51.0	2.38
Z907	16.75	0.686	58.9	6.77

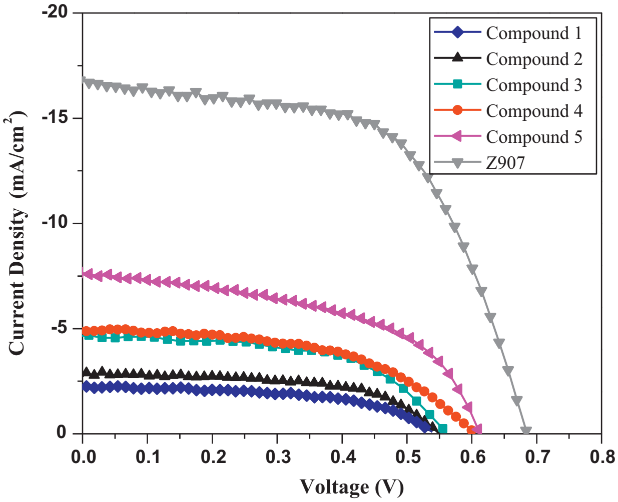

Fig. 5. *J*–*V* characteristics of Dyes **1**–**5** and **Z907**.

The performance of the dye sensitized solar cells (DSSCs) was measured by incident photon-to-current conversion efficiency (IPCE) and photocurrent–voltage (*J*–*V*) measurements. Fig. 5 shows the photocurrent–voltage (*J*–*V*) curve for DSSCs based on five porphyrin dyes (Dyes **1**–**5**). The short-circuit current densities (J_{sc}), open-circuit voltages (V_{oc}), fill factors (*ff*) and power conversion efficiencies (η) of the cells are summarized in Table 1. The Dye **5** gave the best performance, the conversion efficiency (η) arrives at 2.38% with J_{sc} 7.63 mA/cm^2, V_{oc} 0.613 V, *ff* 51.0%, which reaches 35% with respect to **Z907**-based device fabricated under the similar conditions. The highest J_{sc} compared with other devices in this study is attributed to the high extinction coefficient as shown in Fig. 2a. As we know, the aggregation of the dye could decrease V_{oc}, 4-methoxy-triphenylamine moiety as donating group could effectively suppress the dye-aggregation [34]. Otherwise, the increase of the intramolecular charge separation maybe benefit for the increase of V_{oc} [35]. Accordingly, the Dye **5** gave the largest V_{oc}. Therefore, the performance of these dyes is improved due to the

Table 2
Computed excitation energies (eV), oscillation strengths (f) and two highest electronic transition configurations for the optical transitions below 3.2 eV for Dye **2** in THF[a].

No.	Transition energies, nm	Excitation energies, eV[b]	Oscillator strengths, f	Main configurations H = HOMO, L = LUMO, L + 1 = LUMO + 1, *etc.*
1	575.5	2.15	0.0470	H – 0 → L + 0 (+44%); H – 1 → L + 1 (+24%) H – 0 → L + 1 (+23%); H – 1 → L + 0 (+13%)
2	540.8	2.29	0.0663	H – 0 → L + 1 (+40%); H – 1 → L + 0 (+25%) H – 0 → L + 0 (+22%); H – 1 → L + 1 (+12%)
3	408.1	3.04	1.4710	H – 1 → L + 1 (+35%); H – 0 → L + 0 (+12%) H – 1 → L + 0 (+11%)
5	402.3	3.08	1.6885	H – 1 → L + 0 (+34%); H – 0 → L + 1 (+15%) H – 1 → L + 1 (+11%)
6	371.2	3.34	0.0285	H – 0 → L + 2 (+41%); H – 2 → L + 0 (+36%) H – 2 → L + 1 (+15%)
7	368.4	3.37	0.0235	H – 0 → L + 2 (+48%); H – 2 → L + 0 (+27%) H – 2 → L + 1 (+14%)

[a] Calculated using TD-B3LYP/6-31G*//B3LYP/6-31G* and C-PCM framework. See Table S2 for more data on Dyes **1**, **3**–**5** in supporting information.
[b] Excitation energies with oscillation strengths having <0.01 eV are ignored.

increase of the photocurrent and open circuit voltage. We believe that intramolecular charge separation and broad absorption bands with high extinction coefficient is responsible for the significant enhancement of the conversion efficiency.

4. Conclusion

In conclusion, we have successfully designed and synthesized a series of *trans*-D–B–A-porphyrin based dyes with different donor and acceptor groups to fabricate dye-sensitized solar cells. The results of calculation and experiments clearly demonstrate that the band gap can be regulated by increasing the intramolecular charge-separation and introducing different donor and acceptor. Among the five synthesized dye molecules, porphyrin Dye-**5** exhibits the maximum power conversion efficiency (2.38%). Therefore, optimization of these factors is a valid way to improve the performance of solar cells, which provides a revelation to exploit highly efficient porphyrin sensitizers for dye-sensitized solar cell.

Acknowledgments

Authors would like to acknowledge the financial support from Nanyang Technological University (RG50/08) and the Ministry of Education (ARC24/07, no. T206B1218RS), Singapore.

Appendix A. Supplementary data

Supplementary data associated with this article can be found, in the online version, at doi:10.1016/j.jphotochem.2011.01.003.

References

[1] B. Oregan, M. Gratzel, Nature 353 (1991) 737–740.

[2] A. Mishra, M.K.R. Fischer, P. Bauerle, Angew. Chem. Int. Ed. 48 (2009) 2474–2499.

[3] W.M. Campbell, A.K. Burrell, D.L. Officer, K.W. Jolley, Coord. Chem. Rev. 248 (2004) 1363–1379.

[4] H. Imahori, T. Umeyama, S. Ito, Acc. Chem. Res. 42 (2009) 1809–1818.

[5] M.K. Nazeeruddin, A. Kay, I. Rodicio, R. Humphrybaker, E. Muller, P. Liska, N. Vlachopoulos, M. Gratzel, J. Am. Chem. Soc. 115 (1993) 6382–6390.

[6] Q.J. Yu, S. Liu, M. Zhang, N. Cai, Y. Wang, P. Wang, J. Phys. Chem. C 113 (2009) 14559–14566.

[7] P. Wang, S.M. Zakeeruddin, J.E. Moser, M.K. Nazeeruddin, T. Sekiguchi, M. Gratzel, Nat. Mater. 2 (2003) 402–407.

[8] H. Choi, I. Raabe, D. Kim, F. Teocoli, C. Kim, K. Song, J.H. Yum, J. Ko, M.K. Nazeeruddin, M. Gratzel, Chem. Eur. J. 16 (2010) 1193–1201.

[9] G. Zhang, H. Bala, Y. Cheng, D. Shi, X. Lv, Q. Yu, Chem. Commun. 16 (2009) 2198–2200.

[10] W. Zeng, Y. Cao, Y. Bai, Y. Wang, Y. Shi, M. Zhang, F. Wang, C. Pan, P. Wang, Chem. Mater. 22 (2010) 1915–1925.

[11] Y. Wang, W.Q. Deng, X.-W. Liu, X. Wang, Int. J. Hydrogen Energy 34 (2009) 1437–1443.

[12] S. Hwang, J.H. Lee, C. Park, H. Lee, C. Kim, M.H. Lee, W. Lee, J. Park, K. Kim, N.G. Park, Chem. Commun. 46 (2007) 4887–4889.

[13] D.P. Hagberg, T. Edvinsson, T. Marinado, G. Boschloo, A. Hagfeldt, L.C. Sun, Chem. Commun. 21 (2006) 2245–2247.

[14] G.E. Collis, W.M. Campbell, D.L. Officer, A.K. Burrell, Org. Biomol. Chem. 3 (2005) 2075–2084.

[15] K. Hara, M. Kurashige, S. Ito, A. Shinpo, S. Suga, K. Sayama, H. Arakawa, Chem. Commun. 2 (2003) 252–253.

[16] K. Hara, K. Sayama, Y. Ohga, A. Shinpo, S. Suga, H. Arakawa, Chem. Commun. 6 (2001) 569–570.

[17] A.K. Burrell, W.M. Campbell, D.L. Officer, S.M. Scott, K.C. Gordon, M.R. McDonald, J. Chem. Soc. Dalton Trans. 19 (1999) 3349–3354.

[18] J.-L. Song, P. Amaladass, S.-H. Wen, K.K. Pasunooti, A. Li, Y.-L. Yu, X. Wang, W.-Q. Deng, X.-W. Liu, New J. Chem. 35 (2011) 127–136.

[19] M. Tanaka, S. Hayashi, S. Eu, T. Umeyama, Y. Matano, H. Imahori, Chem. Commun. 20 (2007) 2069–2071.

[20] M.K. Nazeeruddin, R. Humphry-Baker, D.L. Officer, W.M. Campbell, A.K. Burrell, M. Gratzel, Langmuir 20 (2004) 6514–6517.

[21] H. Imahori, S. Hayashi, H. Hayashi, A. Oguro, S. Eu, T. Umeyama, Y. Matano, J. Phys. Chem. C 113 (2009) 18406–18413.

[22] S. Hayashi, M. Tanaka, H. Hayashi, S. Eu, T. Umeyama, Y. Matano, Y. Araki, H. Imahori, J. Phys. Chem. C 112 (2008) 15576–15585.

[23] W.M. Campbell, K.W. Jolley, P. Wagner, K. Wagner, P.J. Walsh, K.C. Gordon, L. Schmidt-Mende, M.K. Nazeeruddin, Q. Wang, M. Gratzel, D.L. Officer, J. Phys. Chem. C 111 (2007) 11760–11762.

[24] E.E. Bonfantini, A.K. Burrell, W.M. Campbell, M.J. Crossley, J.J. Gosper, M.M. Harding, D.L. Officer, D.C.W. Reid, J. Porphyrins Phthalocyanines 6 (2002) 708–719.

[25] Q. Wang, W.M. Campbell, E.E. Bonfantini, K.W. Jolley, D.L. Officer, P.J. Walsh, K. Gordon, R. Humphrybaker, M.K. Nazeeruddin, M. Gratzel, D.L. Officer, J. Phys. Chem. B 109 (2005) 15397–15409.

[26] N.K. Subbaiyan, L. Obraztsov, C.A. Wijesinghe, K. Tran, W. Kutner, F. D'Souza, J. Phys. Chem. C 113 (2009) 8982–8989.

[27] N. Kristian, Y.L. Yu, P. Gunawan, R. Xu, W.-Q. Deng, X.-W. Liu, X. Wang, Electrochim. Acta 54 (2009) 4916–4924.

[28] C.W. Lee, H.P. Lu, C.M. Lan, Y.L. Huang, Y.R. Liang, W.N. Yen, Y.C. Liu, Y.S. Lin, E.W.G. Diau, C.Y. Yeh, Chem. Eur. J. 15 (2009) 1403–1412.

[29] J.K. Laha, S. Dhanalekshmi, M. Taniguchi, A. Ambroise, J.S. Lindsey, Org. Process Res. Dev. 7 (2003) 799–812.

[30] (a) M.J. Frisch, et al., Gaussian 03, Revision C.02, Gaussian, Inc., Wallingford, CT, 2004;
(b) R. Dennington, T. Keith, J. Millam, K. Eppinnett, W.L. Hovell, R. Gilliland, GaussView, Semichem, Shawnee Mission, KS, 2003.

[31] S.I. Gorelsky, B.P. Lever, J. Organomet. Chem. 635 (2001) 187–196.

[32] A.D. Adler, F.R. Longo, J.D. Finarell, J. Goldmach, J. Assour, L. Korsakof, J. Org. Chem. 32 (1967) 476–478.

[33] D.P. Hagberg, J.H. Yum, H. Lee, F. De Angelis, T. Marinado, K.M. Karlsson, R. Humphry-Baker, L.C. Sun, A. Hagfeldt, M. Gratzel, M.K. Nazeeruddin, J. Am. Chem. Soc. 130 (2008) 6259–6266.

[34] (a) N. Satoh, T. Nakashima, K. Yamamoto, J. Am. Chem. Soc. 127 (2005) 13030–13038;
(b) N. Satoh, J.S. Cho, M. Higuchi, K. Yamamoto, J. Am. Chem. Soc. 125 (2003) 8104–8105;
(c) Q. Wang, S.M. Zakeeruddin, J. Cremer, P. Bauerle, R. Humphry-Baker, M. Grätzel, J. Am. Chem. Soc. 127 (2005) 5706–5713.

[35] Y. Ooyama, Y. Harima, Eur. J. Org. Chem. (2009) 2903–2934.